7 Tesla magnetic resonance imaging for neurodegenerative dementias in vivo: a systematic review of the literature

Elizabeth F McKiernan[a]*, MBChB, MSc, and John T O'Brien, DM[a]

[a] Department of Psychiatry, Cambridge Biomedical Campus, University of Cambridge, Cambridge, UK.

* Correspondence to: Dr. Elizabeth McKiernan, Department of Psychiatry, School of Clinical Medicine, University of Cambridge, Box 189, Level E4, Cambridge Biomedical Campus, Cambridge, UK, CB2 0SP, Email: em654@medschl.cam.ac.uk

Key words: 7T MRI; neurodegenerative dementia, Alzheimer's disease; Lewy body dementia; frontotemporal dementia; Huntington's disease

Abstract:

The spatial resolution of 7T MRI approaches the scale of pathologies of interest in degenerative brain diseases, such as amyloid plaques and changes in cortical layers and subcortical nuclei. It may reveal new information about neurodegenerative dementias, though challenges may include increased artefact production and more adverse effects.

We performed a systematic review of papers investigating Alzheimer's disease (AD), Lewy body dementia (LBD), frontotemporal dementia (FTD) and Huntington's disease (HD) in vivo using 7T MRI. Of 19 studies identified, 15 investigated AD (the majority of which examined hippocampal subfield changes) and 4 investigated HD.

Ultra-high resolution revealed changes, not visible using lower field strengths, such as hippocampal subfield atrophy in mild cognitive impairment. Increased sensitivity to susceptibility enhanced iron imaging, facilitating amyloid and microbleed examination; for example, higher microbleed prevalence was found in AD than previously recognised. Theoretical difficulties regarding image acquisition and scan tolerance were not reported as problematic. Study limitations included: small subject groups, a lack of studies investigating LBD and FTD, and an absence of longitudinal data.

In vivo 7T MRI may illuminate disease processes, and reveal new biomarkers and therapeutic targets. Evidence from AD and HD studies suggest that other neurodegenerative dementias would also benefit from imaging at ultra-high resolution.

1. Introduction:

Neurodegenerative dementias, including Alzheimer's disease (AD), Lewy body dementia (LBD), frontotemporal dementia (FTD) and the dementia of Huntington's disease (HD) account for the majority of dementia syndromes diagnosed worldwide,[1]. Alzheimer's produces a syndrome characterised by deficits in multiple cognitive areas, including orientation and social function; most often the predominant symptom is of progressive anterograde amnesia,[2]. Diagnostic hallmarks of AD are amyloid plaques and neurofibrillary tangles found at post mortem which typically follow a regional path,[3]. A number of in vivo biomarkers have been described and current recommended criteria for diagnosis of probable AD includes neuroimaging markers of abnormal brain amyloid deposition and neuronal degeneration,[4]. Amyloid deposition can be imaged via increased uptake of amyloid markers on positron emission tomography (PET), such as 11[C]PIB),[5]. Neuronal degeneration in AD can be imaged via decreased uptake of [18]F-FDG PET (an indicator of tissue metabolism) and via structural magnetic resonance imaging (MRI) which shows typical patterns of atrophy in the temporal and parietal lobes,[6].

Features of LBD include the triad of fluctuating cognition, visual hallucinations and extra-pyramidal movement disorder,[7] and is characterised by the presence of abnormal alpha-synuclein in neurons and glial cells found in the brainstem, limbic system and cortex at post mortem,[8]. The most commonly used neuroimaging technique in diagnosis of LBD is dopaminergic imaging of the basal ganglia with sensitivity 87% and specificity 94% for differentiating between LBD/Parkinson's disease dementia (PDD) and other dementia types,[9]. A recent review of LBD imaging described changes identified using MRI including volumetric differences in the substantia innominate and putamen and degeneration of the pons and thalamus,[10].

In FTD episodic memory is relatively preserved; changes in personality, disinhibition and language difficulties predominate. It is characterised by atrophy of frontal and temporal lobes and the histological presence of TDP-43 and/or FUS pathology, and may mimic atypical AD clinically,[11]. A number of in vivo neuroimaging markers have been described, including: atrophy in frontal insula, cingulate, striatum and anterior temporal lobe on structural MRI, frontal lobe hypo-perfusion using arterial spin labelled (ASL) perfusion imaging and reduced fractional anisotropy (FA) in frontal regions using diffusion tensor imaging (DTI),[11].

Huntington's disease is an autosomal dominant trinucleotide repeat disorder with an estimated prevalence of 5.7 per 100,000 in majority Caucasian populations (in whom incidence is highest),[12]. Characterised by the presence of cerebral intranuclear inclusions of mutated huntingtin it produces movement disorder, cognitive decline and behavioural symptoms. Dementia can occur at any point in the disease process and cognitive deficits are primarily in concentration, short-term memory and executive function. Carriers are identified via genetic testing which shows an expansion of CAG trinucleotide repeats within the *Huntingtin* gene on chromosome 4,[13]. A reduction in striatal volume is the most consistent MRI finding in HD and correlates with age at disease onset, duration of disease and CAG repeat length. Changes in caudate and putamen volumes, cortical thinning and white matter (WM) atrophy have also been identified,[14]. A large longitudinal multicenter trial, used 3T MRI to demonstrate progressive grey and white matter, whole brain and regional cortical atrophy in HD and premanifest (prodromal or pre-motor) HD, with the largest effect sizes seen in the caudate and WM,[15].

MRI is an important clinical tool, used to rule-out reversible causes of dementia, and to aid in diagnosis of early dementias or those presenting in an atypical manner,[16]. Neuroimaging dementia research is largely concerned with the discovery of new biomarkers with such aims as: earlier diagnosis, identification of 'at-risk' individuals and those with 'prodromal' dementia syndromes, monitoring of disease progression, and identification of new treatment targets by illuminating the natural history of the disease in vivo. Increasing static field strength (B_0) from 1.5 to 3T has allowed imaging of micro as well as macro-structures in the brain, e.g. not only analysis of whole hippocampal volumes but differentiation between hippocampal subfield volumes in health and disease,[17]. However, even at 3T, MRI voxels typically measure mm, consequently the resulting images remain several orders of magnitude away from the size of pathologies of interest; cortical layers, hippocampal subfields, brainstem nuclei, plaques, tangles and microbleeds are typically measured in μm. Seven tesla MRI may allow increases in image resolution allowing us to visualise these microstructures and pathology in vivo.

Seven tesla MRI creates both opportunities and challenges for the neuroscience community (see Balchandani and Naidich (2015),[18] for a technological summary of 7T MRI capabilities). In theory image resolution increases by around 30% as B_0 increases from 3T to 7T. The relationship between image resolution and B_0 is complex because resolution is determined by a number of factors including signal to noise ratio (SNR), voxel size and image acquisition time. Theoretically, SNR increases linearly with increasing B_0 and should more than double as B_0 increases from 3T to 7T. However, in practice maintenance of field homogeneity becomes more challenging; spatial and intensity distortions occur more commonly as B_0 increases. Contrast between tissue types also determines image resolution

and is influenced by such factors as T1, T2 and T2* relaxation times and sensitivity to susceptibility (phase difference between tissues).

Tissue relaxation values change as B_0 increases: slower and converging for T1 and faster for T2 and T2*. Faster T2* results in better contrast of iron deposits, calcifications and deoxyhaemoglobin, however, drop-out and susceptibility artefacts increase, particularly in brain areas close to bone, vasculature or cerebrospinal fluid (CSF). Sensitivity to susceptibility can be used to measure paramagnetic substances such as iron and increases in proportion to increasing B_0 and longer echo time (TE). Increasing B_0 allows shorter TEs to be used, producing potential improvements in image resolution and shorter acquisition times. Acquisition times are important in dementia imaging as participants may find long scan durations particularly difficult to tolerate and many dementia processes are accompanied by movement disorders. Image acquisition at 7T may require a choice between ultra-high resolution, which is disproportionately adversely affected by head and physiological movement, and faster acquisition times, which may ameliorate the effects of excess motion,[19].

Newly developed technologies and imaging protocols can overcome some of the challenges described above, e.g. advanced B_0 shimming and small voxel volumes have been found to compensate for increased field inhomogeneity. New radio frequency (RF) pulse sequences are also required because as B_0 increases to 7T the wavelength of the RF is close to the diameter of the head leading to signal drop-out and contrast changes in brain peripheries,[18]. Areas of interest in dementia research include small, peripheral brain regions such as the hippocampus, entorhinal cortex (ERC), and amygdala; areas identified to play a large role in post-mortem histological studies,[20]. Due to their small size and complex internal structures

such regions are likely to benefit from higher resolution imaging, however, they are also brain most difficult to examine using MRI due to artefact production.

In humans, potential adverse effects produced by high electromagnetic fields used in MRI include transient effects such as: vertigo, peripheral nerve stimulation, metallic taste in the mouth, and impaired cognition. More serious longer term effects include damage to implanted medical devices such as pacemakers, intracranial clips and neuro-stimulators, which may be damaged directly by the applied magnetic fields or by torque, which may displace devices within the body,[21]. There are limits to the amount of radio frequency (RF) power deposition (specific absorption rate; SAR) that can be applied in human subjects. Specific absorption rate increases proportionally to B_0^2. This large increase in SAR between 3T and 7T means that the number, duration and amplitude of RF pulses that can be applied are restricted, due to heating effects on objects in the scanner bore. These effects may be especially problematic for patient populations being imaged for dementia research, as thermo-regulation may be impaired in people who are older, have health problems or take medications,[22].

The aim of this literature review is to systematically describe and evaluate published studies which have used 7T MRI in vivo in subjects with neurodegenerative dementias. Gaps in the current literature and potential future applications for this technology in neurodegenerative dementias will then be discussed.

2. Methods:

The initial search was completed on PubMed using the following terms: “7T” OR “7 Tesla” OR “seven tesla” OR “ultrahigh resolution” AND “MR” OR “MRI” OR “magnetic resonance

imaging" AND "neurodegen*" OR "Mild cognitive impairment" OR "MCI" OR "Alzheimer's" OR "AD" OR "Lewy body dementia" OR "LBD" OR "Parkinson's disease dementia" OR "PDD" OR "Frontotemporal dementia" OR "FTD" OR "Huntington*" OR "HD". Papers published between 1st January 1985 and 1st December 2016 were searched. These search criteria produced 393 results. Articles reviewed were limited to those related to in vivo human studies and only papers in English were included. Relevant papers were identified by manual review of titles and abstracts. Sixteen relevant studies were identified. The reference lists of these papers were searched to identify further relevant papers and 3 further relevant studies were identified, yielding a total of 19 papers (Figure 1).

Figure 1: Flow diagram depicting the systematic review process.

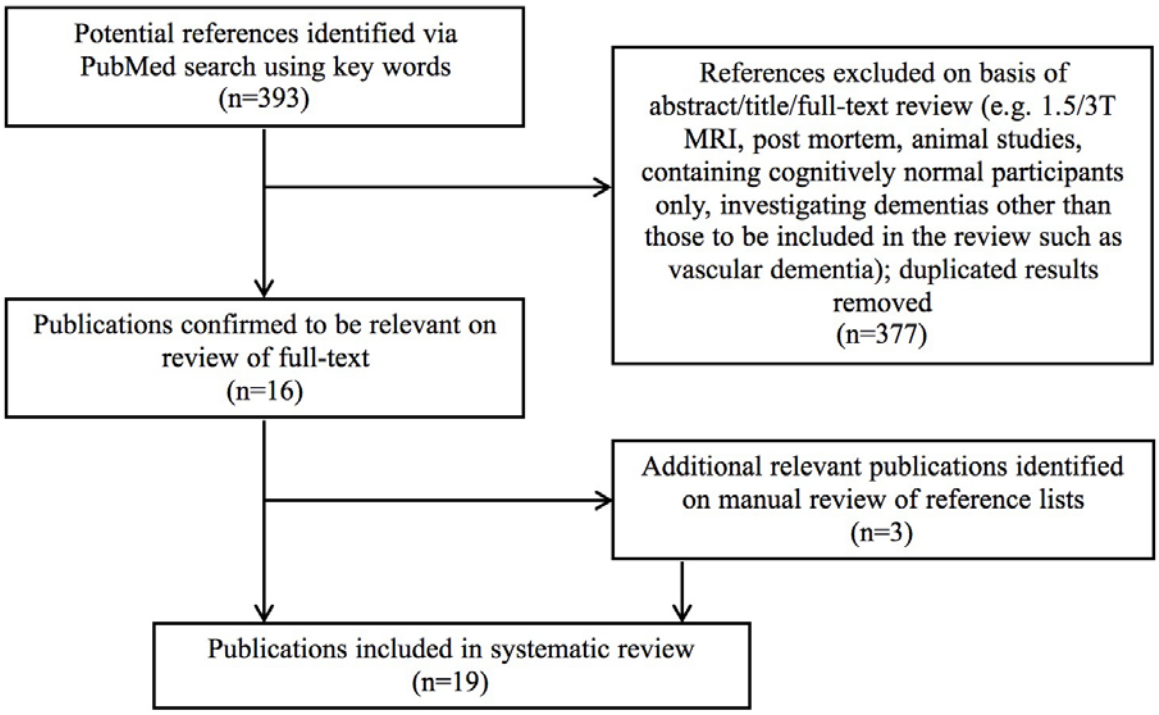

3. Results:

3.1 Alzheimer's disease papers:

Papers identified fell broadly into 4 groups, those reporting medial temporal lobe structures, those reporting vascular changes (microbleeds and microinfarcts), those investigating markers of amyloid and other papers. In all papers AD was defined according to the NINCDS-ADRDA criteria [2, 4] and in studies with a mild cognitive impairment (MCI) group this was defined according to either the NIA-AA criteria,[23] or Petersen criteria,[24]. Additional criteria, such as minimum MMSE score and an adequate level of English comprehension were stipulated in some studies.

Seven in vivo 7T MRI studies including individuals with AD and/ or MCI examining hippocampal volumes and subfields were identified (Table 1). Image acquisition methods were similar across the majority of the studies; T2-weighted Fast/Turbo Spin Echo (FSE/ TSE) acquisition sequences were mostly utilised. Reported in-plane resolutions varied between $0.166mm^2$ and $0.90mm^2$. Segmentation of the hippocampus and its subfields was mostly performed manually based on anatomical landmarks. No papers presented a fully automated approach for subfield segmentation. Papers used various anatomical landmarks for segmentation and differences in approach may explain some current and future variability between findings at 7T. There was consensus between these papers that individual hippocampal subfields can be differentiated using 7T MRI in vivo and that the morphometry of these subfields is altered in AD and may also be altered in MCI. There was not consensus within the literature regarding which layers are most affected and in what ways, the most commonly reported area affected in AD was the cornu Ammonis layer 1 (CA1, specifically the strata radiatum, lacunosum and moleculare (CA1-SRLM)). Volume reductions in this

subfield were seen consistently in early AD and correlations between CA1 width and delayed recall memory performance were found,[27-30].

Eight other in vivo 7T MRI studies including individuals with AD and/ or MCI were identified (Table 2). Four papers investigated amyloid plaque deposition, 1 paper investigated microbleed prevalence, 1 paper investigated microinfarct prevalence, 1 paper investigated perivascular density and 1 paper addressed movement artefact reduction within the MRI scanner. The studies investigating amyloid plaque deposition used T2*-weighted gradient echo (GRE) acquisition sequences. Reported in-plane resolutions varied between $0.156mm^2$ and $0.5mm^2$. At such resolutions it is not possible to visualize the majority of amyloid plaques directly; their mean diameter being in the tens of μm[44]. Various methods were used to image amyloid; susceptibility weighted imaging (SWI) was used to directly visualise *"senile-plaque-like-pathology"*, small hypo-intense areas, in the parietal cortex,[36], a finding which was not replicated elsewhere,[40]. Increased phase shift (seen in the presence of iron which co-localises with amyloid) was found in AD throughout the cortex though not in the hippocampi,[40-41]; in addition this effect was found to be greater in early onset AD than late onset AD,[41]. Raised quantitative susceptibility mapping values (QSM; used as a proxy for cortical iron burden) was found to colocalise with Aβ-plaque-load (measured using C[11]-PiB-PET) in APOE e4-positive MCI but not in the APOE e4-negative MCI or in APOE e4-positive controls,[38].

Only 1 paper directly compared results obtained using 7T and 3T MRI,[32]; statistically significant differences in microbleed prevalence were seen between controls and AD/MCI using 7T only.

Only 2 papers commented on tolerability of the scan and adverse effects,[26-27]; one reported a single case of tinnitus,[26] and the other reported no significant adverse effects,[27].

Table 1: Hippocampal volumes and subfield papers. 7T MRI in vivo studies including subjects with neurodegenerative dementia.

Paper	**Imaging methods**	**Participants**	**Question**	**Results**
Boutet et al. (2014)[25]	Whole brain: MP-RAGE acquisition; 176 slices; voxel size 0.9x0.9x0.9mm Hippocampus: 2D T2* GRE acquisition; 3x15 slices; voxel size 0.3x0.3x1.2mm Manual segmentation based on anatomical landmarks	NC = 7 'mild to moderate' AD* = 4	Can volume changes in distinct hippocampal layers be detected in vivo using 7T MRI (using an imaging protocol which distinguishes between layers richer or poorer in neuronal bodies)?	Bilateral reduction of CA-SRLM and SUB-SP volumes (sig) in AD (average difference in cross-sectional ranges from -29 to -49%) Trend towards reduction of left CA-SP in AD (non-sig)
Kerchner et al. (2010)[26]	Whole brain: T1-weighted 3T MRI MTL: 2D T2*-weighted GRE acquisition; 100 slices in 15 subjects and 40 slices in 15 subjects; slice gap 0mm in 15 subjects and 3mm in 15 subjects; voxel size 0.195x0.195x2mm; scan time 9.6min Manual segmentation based on anatomical landmarks	NC = 16 'Mild' AD*** = 14	Can tissue loss in the CA1 apical neuropil layer of the hippocampus be seen on MRI in vivo in mild AD?	CA1 cell-body layer thickness and entire CA1 subfield thickness not sig diff between groups CA1-SRLM width decreased in AD (sig) CA1 apical neuropil thickness decreased in AD (sig) Left lateralised changes in AD THV not sig diff between groups (measured at 3T)
Kerchner et al. (2012)[27]	MTL: T2-weighted FSE acquisition; 16-18 slices; voxel size 0.166x0.166x1.5mm (interpolated reconstruction from 0.22x0.22x1.5mm acquired voxels); scan time around	Mild AD** = 9	Do hippocampal subfield widths correlate with performance on episodic memory tasks?	Relayed recall performance (DRP) correlated with CA-SRLM width r2=0.69; with CA1-SP width r2=0.5; with width of ERC r2=0.62 (all sig) Differences between groups left lateralised

	10min Manual and semi-automated segmentation based on anatomical landmarks			
Kerchner et al. (2013)[28]	As per [27]	YNC = 9 ONC = 18 MCI† = 15 AD** = 11	Do ERC and CA1-SRLM share an early vulnerability to AD pathology? (Does atrophy occur in a proportional manner between the two structures?)	Ratio of CA1-SRLM to ERC width 0.25+/-0.03 across all subjects Width of CA1-SRLM and of ERC decreased as a function of age and of cognitive impairment CA1-SRLM width correlated with episodic memory performance in AD and aMCI groups but not in controls ERC width correlated with episodic memory performance in AD group (and shows non-significant trend in aMCI) Correlation between ERC and CA1-SRLM and between ERC and CA1-SP sig when THVs controlled for ERC and CA1-SRLM share vulnerability to both age and AD-associated atrophy
Kerchner et al. (2014)[29]	As per [27]	NC = 14 MCI† = 14 AD* = 11	Is there a relationship between APOE e4, hippocampal subfield morphology and episodic memory?	APOE e4 load associated with thinning of CA1-SRLM (sig) and with poorer performance on episodic memory tasks (an association was not seen with other areas of cognitive examination). The association persisted after controlling for dementia severity APOE e4 was not associated with changes in other hippo subfields or ERC
Wisse et al. (2014)[30]	MTL: 3D T2-weighted TSE (whole brain) acquisition; voxel size 0.35x0.35x0.7mm; scan time 10:15min Manual in-house segmentation approach	NC = 29 MCI†† = 16 AD* = 9	Do hippo subfield and ERC volumes differ between NC, MCI and AD groups? Do hippo subfield and ERC volumes correlate with age in NCs?	ERC, SUB, CA1, CA3, DG&CA4 and THV volumes smaller in AD than NC (sig). ERC, SUB, CA1, DG&CA4, and THV volumes smaller in AD than MCI (sig) MMSE correlated with ERC, SUB, CA1, DG&CA4 volumes (sig) CA1, DG&CA4 and THV volume loss correlated with increasing age (sig)

Wisse et al. (2015)[31]	Hippocampal formation: 7T 3D T2-weighted TSE (whole brain) acquisition; voxel size 0.35×0.35×0.7mm; scan time 10:15min ICV: 3T T2-weighted fast field echo; voxel size 3×0.99×0.99mm; scan time 2:48min Diffusion data: 3T single-shot spin echo planar imaging sequence (SENSE) (twice-refocused); voxel size 2.5x2.5x2.5mm; scan time 5:32 min Manual in-house segmentation approach	NC = 17 MCI†† =15 mild AD* = 10	Does ERC and hippocampal degeneration induce degeneration of their associated WM tracts (fornix and parahippocampal cingulum)?	Fornix FA lower in AD (sig) CA1, DG&CA4, SUB volume lower in MCI and AD (sig) Fornix FA associated with SUB volume β=0.53 (sig) in MCI/AD. Fornix FA not associated with ERC or other hippo subfield volumes in MCI/AD PHC FA not associated with ERC or other hippo subfield volumes in MCI/AD Hippo subfield atrophy not associated with reduction in whole brain WM FA

Key for tables 1 and 2: AD diagnostic criteria used: *[2], **[4], ***criteria not specified; MCI diagnostic criteria used: †[23], ††[24], ††† criteria not specified; AD = Alzheimer's dementia; NC = cognitively-normal controls; ONC = older cognitively-normal controls; YOC = younger cognitively-normal controls; EOAD = early onset Alzheimer's dementia; LOAD = late onset Alzheimer's dementia; MCI = mild cognitive impairment; CA = cornu Ammonis; SRLM = strata radiatum, lacunosum and moleculare; SP = stratum pyramidale; DG = dentate gyrus; SUB = subiculum; hippo = hippocampus; THV = total hippocampal volume; ERC = entorhinal cortex; MTL = medial temporal lobe; ICV = intracranial volume; PHC = parahippocampal cingulum; TMP = temporoparietal region; WM = white matter; GM = grey matter; MRI = magnetic resonance imaging; rs-fMRI = resting state functional MRI; TE = echo time, RF = radio frequency; B_0 = static field strength; 1.5/3/7T = 1.5/3/7 tesla; FA = fractional anisotropy; GRE = gradient echo sequence; FSE/TSE = Fast/Turbo Spin Echo (these terms are synonymous); MP RAGE = magnetization-prepared rapid acquisition gradient echo; QSM = quantitative susceptibility mapping; C[11]-PiB = Carbon 11 Pittsburgh B compound (binds to amyloid); SWI = susceptibility weighted imaging; SPACE = sampling perfection with application optimized contrasts by using different flip angle evolutions; sig = significant ($p<0.05$); ROI: region of interest

Table 2: microbleed, plaque and miscellaneous papers. 7T MRI in vivo studies including subjects with AD.

Paper	Imaging methods	Participants	Question	Results
Microbleed and microinfarct papers:				
Brundel et al. (2012b)[32]	7T MRI: dual-echo 3D T2*-weighted acquisition; voxel size 0.5x0.5x0.7mm 3T MRI: 3D T2*-weighted acquisition; voxel size 0.99x0.99x3mm Visual identification of	NC = 18 AD*/MCI†† = 18	What is the actual prevalence of microbleeds in AD/MCI?	At 7T MRI >= 1 microbleeds in 78% of AD/MCI vs 44% NC (sig) At 3T MRI >=1 microbleeds in 33% of AD/MCI vs 17% NC (non-sig) Higher quantity of microbleeds in AD/MCI (max 80 in one

	microbleeds (MARS criteria,[33])			subject) than NC (max 5 in one subject) (at 7 T) (sig)
van Veluw et al. (2014)[34]	3D FLAIR acquisition; voxel size 0.8x0.8x0.8mm 3D T2-weighted acquisition; voxel size 0.7x0.7x0.7 3D T1-weighted acquisition; voxel size 1.0x1.0x1.0mm 3D dual-echo gradient echo acquisition; voxel size 0.5x0.5x0.7mm Visual identification of microinfarcts described in ref,[35]	NC = 22 AD*/aMCI†† = 29	Are cerebral microinfarcts (CMI) increased in aMCI/AD?	CMIs were found in 45% NC and 55% aMCI/AD (non-sig) No significant difference between CMIs in aMCI and AD groups In all subjects CMIs were uniformly distributed throughout the cortex No relationship between MTL atrophy or MMSE and number of CMIs
Amyloid plaque papers:				
Nakada et al. (2008)[36]	Parietal association cortex SWI: T2*-weighted 2D GRE acquisition; voxel size 0.156×0.156×3mm; scan time 3:48min Visual identification of plaques –described in,[37]	ONC = 10 YNC = 20 AD* = 10	Can senile plaques be visualised using 7T MRI in vivo in AD?	Hypo-intense *"black dots"* representing *"senile-plaque-like-pathology"* seen throughout parietal cortex in 10/10 AD, in 2/10 ONC, and in 0/20 YNC Difference between YNC and ONC, and between AD and ONC (Ryan multiple comparison) sig
van Bergen et al. (2016a)[38]	Structural: T1-weighted MP2RAGE acquisition; voxel size 0.6x0.6x0.6mm; scan time 7:50min QSM: 3D GRE acquisition with 3 echoes; voxel size 0.5x0.5x0.5mm; scan time 13:48min rs-fMRI: 3D T2-prep GRE acquisition; voxel size 1.5x1.5x1.5mm; scan time 7:03min Also: C[11]-PiB-PET QSM maps created in multiple steps - Laplacian based phase unwrapping converted to frequency shift images (in Hz), inverse dipole calculation used to obtain susceptibility maps, values reported relative to reference CSF,[39] rs-fMRI images created using SPM12 (http://www.fil.ion.ucl.ac.uk/spm/)	NC = 22 (7 APOE e4 positive) MCI†† = 15 (6 APOE e4 positive)	What is the relationship between cerebral iron (measured using QSM) MCI and APOE-e4 status? What are the relationships between cerebral iron burden, Aβ - plaque density and MPFC-coupling (measured using rs-fMRI)?	APOE e4 associated with increased cortical iron and higher Aβ-plaque-load in MCI (sig) but not in NC High iron burden in MCI associated with increased MPFC-coupling in ROIs including cingulate and para-cingulate gyri and frontal regions (sig). Within areas of increased MPFC coupling iron-burden and Aβ-plaque-load correlate (sig).
van Rooden et al. (2014)[40]	T2*-weighted 2D GRE acquisition; 20 slices; voxel	NC = 15 AD* = 16	Can amyloid plaques be visualised in the	No focal hypo-intensities found.

	size 0.24x0.24x1mm (FOV included frontal and parietal regions); scan time approximately 10min Hippocampus: 2D T2*-weighted GRE acquisition; 32 slices; voxel size 0.5x0.5x3mm; scan time approximately 6min Visual identification of plaques. Phase shift values for 4 different ROIs (right and left TMP, frontal, and parietal) averaged and phase shift with subcortical WM calculated		cerebral cortex using 7T MRI in vivo in AD?	Increased cortical phase shift in the cortex of the left TMP (AD=0.90, NC=79), right TMP (AD=0.97, NC=0.85), frontal (AD=0.70, NC=0.62), and parietal region (AD=0.87, NC=0.74) in AD (all sig) No phase shift difference between groups in the hippo (left hippo AD=0.09, NC=0.07; right hippo AD=0.10, NC=0.08 (all non-sig)) Association between whole brain phase shift and MMSE scores r=-0.54 (sig)
van Rooden et al. (2015)[41]	T2*-weighted 2D GRE acquisition; 20 slices; voxel size 0.24x0.24x1mm; scan time approximately 10min (FOV included frontal and parietal regions) Phase shift values for 4 different ROIs (right and left TMP, frontal, and parietal) averaged and phase shift with subcortical WM calculated	NC = 27 EOAD* = 12 (onset before 65yr) LOAD* = 17 (onset after 65yr)	Does amyloid deposition (measured as per van Rooden et al. (2014)) differ between EOAD and LOAD?	LOAD and EOAD have increased cortical phase shift values compared to NC in right TMP (LOAD=1.23, EOAD=1.31, NC=0.98), left TMP (LOAD=1.18, EOAD=1.25, NC=0.96), frontal (LOAD=1.04, EOAD=1.15, NC=0.88), parietal (LOAD=1.16, EOAD=1.27, NC=0.98) regions and whole brain (LOAD=1.15, EOAD=1.25, NC=0.95) The differences in all regions and whole brain were significant between NC and LOAD, between NC and EOAD, and between LOAD and EOAD groups
Miscellaneous papers:				
Cai et al. (2015)[42]	T2-weighted 3D TSE SPACE acquisition; 224 slices; voxel size 0.4x0.4x0.4mm; scan time approximately 7.5min (interpolated reconstruction from 0.42×0.42x1mm acquired voxels) PVS automatically segmented using MATLAB	NC = 3 AD*** = 5	Can perivascular spaces (PVS) be imaged and quantified using 7T MRI in vivo?	Increase in PVS density in AD compared to NC (AD=8.0, NC=4.9) (sig)
Versluis et al. (2010)[43]	T2*-weighted acquisition with additional navigator echo technique application; 20 slices; voxel size 0.24×0.24×1mm; scan time approximately 10min	NC = 5 AD*** = 5	What are the sources of additional imaging artefacts seen in AD? Does the application of an additional navigator echo technique	Artefacts produced in AD group by increase in f0 variations (physiological e.g. due to chest volume changes with breathing) and large jumps (caused by movement)

			correct for the increased artefact production?	Application of navigator echo technique corrected for these increased f0 variations and improved image quality and reduced ghosting in 9/10 AD scans

See key below Table 1

3.2 Huntington's disease papers:

Four in vivo 7T MRI studies including individuals with HD and/ or pre-manifest HD were identified (Table 3). Definitions of HD and premanifest HD were not consistent within these papers. In all cases patients were positive for HD mutation with ≥40 CAG repeats, however divisions between premanifest HD and HD were defined according to Unified Huntington's Disease Rating Scale (UHDRS,[53]) motor score and various cut-off values were chosen.

Two papers measured iron deposition in basal ganglia structures, 1 paper investigated changes in the blood brain barrier (BBB), and 1 paper reported on a quantitative textural analysis. As in the AD amyloid-deposition papers described above, the HD papers investigating iron deposition used T2*-weighted gradient echo (GRE) acquisition sequences and reported in-plane resolutions of $0.5mm^2$ and $1mm^2$. Image susceptibility increases in the caudate nucleus (suggesting greater iron deposition) were reported in premanifest HD,[45, 47] and were found to correlate with CAG-Age Product Scaled score (CAPs score,[54] used to estimate the probability of progression to clinical HD within 5 years).

One paper commented on scan tolerability and adverse effects,[45]; in this study 6 participants (3 patients and 3 controls, 20% of participants) were excluded as they did not tolerate 7T MRI, however, the reasons behind this were not elaborated on.

Table 3: 7T MRI in vivo studies including subjects with HD and pre-manifest HD.

Paper	Imaging methods	Participants	Question	Results
Apple et al. (2014)[45]	Volumetric: inversion recovery T1-weighted acquisition; voxel size 1x1x1mm; scan time 3:33min Phase imaging: GRE acquisition; voxel size 0.5x0.5x4mm Also 3T volumetric T1-weighted acquisition; scan time 6:18 min Phase images constructed with fully automated phase unwrapping algorithm,[46]	NC = 13 PreHD† = 13 (originally 16 per group - 6 excluded due to not tolerating MRI)	Do quantitative 7TMR phase measurements of 7T LFS within CN differ between groups?	Higher CN LFS in Pre-motor HD vs NC (sig) Strong correlation between LFS and CAPs score (R^2=0.61, sig)
van Bergen et al. (2016b)[47]	T1-weighted MP-RAGE acquisition; voxel size 0.6x0.6x0.6mm; scan time 6:32min QSM: multi-echo 3D GRE acquisition; voxel size 1x1x1mm; scan time 6:12min QSM maps created in multiple steps - Laplacian based phase unwrapping converted to frequency shift images (in Hz), inverse dipole calculation used to obtain susceptibility maps, values reported relative to reference region (CSF in lateral ventricles)[39] R2* maps calculated using the power method,[48]	NC = 16 PreHD††† = 15	Do groups show differences in magnetic susceptibility (proxy measure of iron deposition) in basal ganglia structures in vivo using QSM and R2* at 7T MRI?	Increased magnetic susceptibility in CN and putamen (around 2x (sig)) in preHD (correlation with CAPs score and significant reductions in volume) Increased magnetic susceptibility in GB (sig) in preHD Decreased magnetic susceptibility in SN and hippocampus (sig) in preHD Increased R2* values in CN and putamen in preHD (sig), however findings only in these 2 regions and effect size smaller
Doan et al. (2014)[49]	3D T1-weighted GRE acquisition; voxel size 0.3x0.3x2mm 3D T2*-weighted GRE acquisition; voxel size 0.25x0.25x0.5mm Also 3T T1-weighted	NC = 5 HD = 8* PreHD†† = 7	Are there textural differences in subcortical structures between groups?	No significant differences between textural features in subcortical structures in preHD and NC when Bonferroni applied. Without correction for multiple comparisons differences seen in CN (sig) Difference between textural features in putamen in HD vs NC

	volumetric acquisition; 164 slices; voxel size 1.1x1.0x1.0mm Textural features analysed in ROIs using 3D Gray-Level Co-occurrence Matrix,[50]			when Bonferroni applied (sig). Without correction for multiple comparisons differences seen in the pallidum, CN , putamen and thalamus (all sig)
Drouin-Ouellet et al. (2015)[51] NB/ Expansive study utilising mouse model, 3T and 7T MRI and post mortem tissue analysis. 7T MRI part of paper examined here.	LL-EPI F-SAIR ASL acquisition protocol; voxel size 2x2x4mm PSIR anatomical acquisition; voxel size 0.8x0.8x0.8mm Turbo field EPI (MR angiogram); 100 slices; 0.6x0.6x0.6mm Average aCBV (ml blood/100ml tissue) and arterial transit time calculated using 2 compartment vascular kinetic model,[52]	In 7T part: NC = 7 HD** = 8	Are differences in aCBV (representing changes in cerebral vasculature) seen between groups?	Increase in cortical GM aCBV in HD (sig) No correlation between aCBV and GM volume No difference in aCBV in caudate or putamen.

Key for table 3: HD = Huntington's disease; PreHD = premanifest HD; NC = cognitively-normal controls; HD diagnostic criteria used: positive for HD mutation with ≥40 repeats and * Unified Huntington's Disease Rating Scale (UHDRS) motor subscale score ≥5, ** no UHDRS motor score cut-off; PreHD diagnostic criteria used: positive for HD mutation with ≥ 40 repeats and † (UHDRS) motor subscale score ≤3, ††UHDRS motor subscale score ≤5, ††† UHDRS motor subscale score ≤15; MRI = magnetic resonance imaging; EPI = echo planar imaging; GRE = gradient echo sequence; MP2-RAGE = magnetization-prepared 2 rapid acquisition gradient echo; LL-EPI F-SAIR ASL = Look-Locker echo planar imaging flow-sensitive alternating inversion recovery arterial spin labelling (used to generate arterial cerebral blood volume maps); LFS = local field shift (a measure of phase and proxy measure of iron deposition); PSIR = phase sensitive inversion recovery; CAPs score = CAG-Age Product Scaled score; R2* = apparent spin-spin relaxation rate; aCBV = arterial cerebral blood volume; GM = gray matterCN = caudate nucleus; GB = globus pallidus; SN = substantia nigra; sig = significant ($p<0.05$);

4. Discussion:

4.1 Hippocampal subfield papers investigating AD/ MCI:

The hippocampus is not a uniform structure, it consists of multiple subfields (CA-1, 2, 3 and 4, subiculum and dentate gyrus,[55]). Post mortem studies suggest early involvement of entorhinal cortex (ERC), subiculum, CA1 and dentate gyrus in AD,[56] and hippocampal atrophy is well established as a biomarker for AD,[57]. It is possible to delineate the subfields of the hippocampus using 3T MRI in vivo; at 1.5T and 3T CA1, CA2 and subiculum atrophy

(using both field strengths to image the same participants) was found in AD but not in MCI,[17]. In this paper improved SNR and greater effect sizes were noted at 3T (compared to 1.5T), suggesting that a similar further improvement might be seen with an increase of B_0 to 7T. Papers reviewed here found atrophic changes in MCI compared to controls,[28, 30-31], suggesting that improved resolution, SNR and consequent increased effect size has real benefits; allowing differentiation of MCI as well as AD from controls at 7T. Changes in CA1-SRLM width in mild AD in the absence of differences in total CA1 or total hippocampal widths were also reported; possibly demonstrating very early changes, previously undetected on MRI,[26]. The average between group difference in CA1-SRLM in this paper was around 1 voxel therefore, at the limit of detectable changes, further emphasising the advantages of 7T MRI. Mild cognitive impairment is of particular interest in AD research; accurate identification of which in this group develop AD may allow earlier diagnosis and allow the targeted treatment of 'prodromal AD', before substantial memory and functional deficits are apparent.

As suggested by post mortem findings, the papers reviewed here consistently report reductions in CA1 (specifically CA1-SRLM), however there was less consensus regarding changes in other subfields. For example, Kerchner et al. (2010) found that hippocampal volume reductions were restricted to CA1-SRLM,[26], while Wisse et al. (2014) noted volume reductions throughout the majority of subfields,[30]. Imaging protocols were reported to be similar in these studies; differences in segmentation approaches, different degrees of dementia and small numbers of subjects may account for the lack of consensus. There is consensus in the papers reviewed that 7T MRI produces images of sufficiently high resolution to allow improved visualisation of hippocampal sub-structures in vivo. However, while high in-plane resolution allowed visualisation of the fine detail of the hippocampal

formation, due to the trade-off between high in-plane resolution and slice thickness, it was not possible to use differences in microstructure to segment the hippocampal formation throughout the length of the hippocampus in vivo. Protocols described in the papers above resorted to macro rather than microstructure to differentiate between some of the subfield layers,[e.g. 31].

Most of the studies reviewed described their participants as ‘mild’ or ‘early’ AD and many stipulated that all participants have a minimum MMSE of 20. This is likely due to the practicalities of imaging subjects with more advanced AD (issues include consent, compliance and excessive within-scanner movement) and may mean that results are not generalisable to the wider patient population. Versluis et al. (2010) suggested that the challenge of increased artefact production due to movement can be largely overcome by modifications of image acquisition sequence and in post-processing,[43]. A navigator echo was used, whereby physiological movement such as that caused by respiration and pulse, is tracked using additional RF-pulses and a correction for this is factored in when the MRI signal is converted into k-space. Excessive motion artefact can also be corrected prospectively, e.g. using an optical tracking system whereby a marker is attached to a dental plate which is held in the subject’s mouth,[58]. However, such methods require an extremely cooperative participant and may be uncomfortable; for patient participants in dementia studies such methods may not be ideal.

None of the reviewed papers reported serial MRI changes at 7T which is an established biomarker for clinical trials,[59]. A lack of longitudinal data limits our understanding of how the changes seen relate to the natural history of these diseases. For example, Wisse et al. (2015) investigated whether ERC and hippocampal degeneration induced degeneration of

associated WM tracts,[31] however investigating the likely order of events within a disease process without using longitudinal data means that conclusions are difficult to reach, in this paper it is possible that WM tracts degenerate first causing associated cortical tissue regions to atrophy in a proportional manner.

Hippocampal subfield pathology is also reported in Parkinson's disease (PD), PDD and LBD. On post mortem, hippocampal pathology is seen primarily in CA2, CA3 and dentate gyrus, rather than CA1 which is primarily affected in AD,[60]. Findings from in vivo MRI studies are conflicting; at 1.5T MRI atrophy has been reported in CA1 and subiculum in LBD compared to controls,[61]. At 3T CA1 has been found to be relatively preserved in LBD compared to AD and not to differ significantly from controls, while significant reductions have been found in whole hippocampal volumes and in CA2-3 in both LBD and AD compared to controls,[62]. The differentiation between hippocampal subfields on MRI has proven difficult at 1.5T and 3T,[63] which may account for differing results between studies. 7T MRI, which begins to approach the scale required to illuminate the histological changes seen in post mortem studies, may be beneficial in confirming to what extent hippocampal subfield volume measurements differ between AD, LBD and controls. In this review we did not identify any published studies examining hippocampal subfields in LBD or FTD using 7T MRI.

4.2. Amyloid plaque studies investigating AD/ MCI:

Amyloid plaques are a cardinal feature of AD, seen initially in the basal neocortex and later widely distributed throughout the cortex,[3]. Positron emission tomography has been highly successful in imaging neural amyloid deposition using such amyloid-binding ligands as 11[C]PiB,[64]. One major advantage of developing a method of imaging amyloid using in

vivo MRI lies in its much higher spatial resolution; specific identification of where in the brain amyloid is deposited at each stage of the disease process may be possible.

Amyloid plaques have high iron content, produce free-radicals and include iron-containing activated microglia; the 7T in vivo plaque studies in this review exploited the increased sensitivity to susceptibility effect seen in brain tissues with abnormal quantities of amyloid. These papers concluded that the most likely origin of directly visualised hypo-intense areas and increased regional phase-shift was amyloid, and this was supported somewhat by the only paper identified in which C[11]-PiB-PET was performed alongside susceptibility-weighted MRI,[38]. In van Bergen et al. (2016a), in APOE e4-positive individuals with MCI, brain regions with high susceptibility sensitivity (considered to reflect neural iron load) on MRI also had increased amyloid on PET. However, a more general correlation between susceptibility effects and amyloid across groups was not reported; an association was found between amyloid deposition and APOE e4 status but not between iron and MCI independent of APOE e4 status. This may suggest that iron and amyloid are independently involved in the disease process. Post mortem studies correlating susceptibility-weighted 7T MRI with histological staining for iron in the same samples report inconsistent findings, correlation between MRI hypo-intensities is reported with both amyloid deposits,[65] and with microscopic iron and activated microglia,[66]. Consequently, explanations other than (or in addition to) amyloid should also be considered; susceptibility effects are also produced by iron, haemosiderin, deoxyhaemoglobin, methaemoglobin, free radicals and free oxygen,[36], it may be that changes in these substrates produced the effects seen independently of amyloid burden and may be implicated in the AD disease process. Findings from histological studies suggest that changes in iron deposition and distribution may also play a key role in AD

pathology,[67]. Disorders of iron homeostasis have also been postulated in PD and related disorders,[68] and FTD[69] .

4.3. Microbleed and microinfarct papers investigating AD/ MCI:

Advantages of 7T over 1.5T MRI in the direct visualisation of microbleeds has been demonstrated; microbleeds were detected in significantly more patients with atherosclerotic disease using 7T MRI (50% of subjects) than using 1.5T (21% of subjects),[70]. A review of 1.5T MRI studies suggested that microbleed prevalence in AD is around 23%,[71]; imaging at both 3T and 7T in the same subjects, Brundel et al. (2012) reported a microbleed prevalence of 33% in AD at 3T (difference from controls was not significant), and of 78% at 7T (with a significant difference between AD and control groups),[32]. The increase in in-plane resolution was from 0.99x0.99mm at 3T to 0.5x0.5mm at 7T. This paper suggests that increasing B_0 to 7T allows the visualisation of pathology not previously evident via MRI.

Histopathology and ex vivo 7T MRI studies suggest an increased prevalence of microinfarcts in AD brains compared with those of controls,[72]. No such significant difference was found between AD and controls using 7T MRI in vivo,[34] which may be accounted for by differences in subject characteristics. Participants in van Veluw et al. (2014),[34] had a minimum MMSE of 20/30 while post mortem subjects are likely to have died with more advanced AD. Including subjects with more advanced disease or longitudinal analysis is required to illuminate the true prevalence of microinfarcts in AD and how they contribute to the clinical presentation. There are implications for our understanding of AD pathology and for AD diagnosis if 7T ‘reveals’ changes not previously visible. For example, the current diagnostic criteria preclude the diagnosis of AD in the presence of extensive infarcts or

microbleeds,[4]and at present individuals with microbleeds or microinfarcts may be excluded from AD studies[32, 71].

4.4. Ultra-high resolution MRI papers investigating HD/ premanifest HD:

The 7T in vivo HD studies investigating iron deposition in premanifest HD,[32, 45] used techniques similar to those described above for imaging amyloid and microbleeds in AD and MCI. Findings suggesting increased neural iron in basal ganglia structures including the caudate nucleus mirror those found at lower field strengths, and at post mortem,[73]. While using susceptibility effects as a proxy for iron burden corresponds well to prior post mortem findings, susceptibility effects in MRI may be caused by a number of different substrates as described above. Calculating apparent spin-spin relaxation rate (R2*) has been validated as a quantitative measure of iron in brain tissues,[74]; as R2* signal increases with B_0, this is a further potential benefit of 7T imaging. van Bergen et al. (2016b) reported increased R2* values in the caudate and putamen in premanifest HD, but not in other basal ganglia structures and effect sizes were smaller than those seen when using QSM,[47]. This might indicate that iron is only one contributor to the susceptibility effects seen in the basal ganglia in this study, the authors suggest demyelination may also contribute. Many of the papers included in this review have benefitted from the increased sensitivity to susceptibility seen at 7T and have used this effect to variously measure amyloid, microbleeds and iron deposition. That the same or similar techniques, including QSM, SWI, R2* and phase shift have been used to measure different processes is problematic, implying a lack of consensus regarding which pathological processes are actually producing changes in these measures on MRI. Ongoing research comparing histological findings, post mortem MRI and polymodal imaging (e.g. comparing amyloid PET with ultra-high resolution MRI) may provide future clarification.

A major limitation of HD papers in this review is the variable definition of premanifest HD vs HD. Each HD paper utilised different UHDRS motor score cut-off values; a lack of consistency within the literature complicates between-paper comparison, and makes it difficult to correlate MRI biomarkers with clinical findings.

4.5. Ultra-high resolution imaging in dementias other than AD and HD:

No in vivo studies using 7T MRI in neurodegenerative dementias other than AD or HD were identified in this review. Proportionally more dementia cases are identified as LBD on post mortem than are diagnosed clinically,[75],suggesting that LBD is under-recognised and may benefit from the identification of biomarkers to facilitate diagnosis in life. A lack of 7T MRI LBD studies may reflect the novelty of 7T MRI, the dominance of AD research, the relatively few individuals diagnosed with LBD compared to AD, or the specific difficulties of imaging in this patient group, in which fluctuating alertness and movement disorders are core clinical features.

Post mortem and imaging studies have identified changes in small, complex brain structures in LBD, e.g. in hippocampal subfields, substantia innominate, putamen, pons and thalamus,[10, 61]. Similar to the hippocampus, the thalamus is extremely complex structurally and success has been reported in differentiating its substructure using 7T MRI in cognitively-normal subjects,[76]. The AD studies in this review suggest that the challenges of imaging small, peripheral brain areas can be overcome with specialised acquisition sequences; increased ghosting, artefacts, and image drop-out do not appear to be as problematic as predicted. This suggests that areas of interest in LBD, such as the thalamus and basal ganglia, may benefit from 7T imaging in a similar way.

No FTD studies were identified in this review. Although less common than AD or LBD, FTD is particularly important clinically due to its over-representation in younger-onset dementias,[77]. The heterogeneous nature of FTD both clinically and pathologically, and the relatively small numbers of individuals affected by this type of dementia may contribute towards this deficit. Distinct atrophic changes in the frontal and anterior temporal lobes is described for all subtypes at 1.5 and 3T,[78]. As is the case for AD and LBD, imaging at ultra-high resolutions may be beneficial in describing the disease processes more fully in vivo and in developing biomarkers that can be used to monitor disease progression, guide prognosis, and be used to evaluate the effects of any potential treatments.

5. Conclusions:

This systematic review identified 19 papers using 7T MRI in vivo to investigate neurodegenerative dementias. Fifteen of the papers identified were concerned with AD and the majority investigated hippocampal subfields. Four of the papers identified were concerned with HD and/ or premanifest HD. The papers in general have four main limitations: firstly, participant numbers are small which limits the power of these studies; secondly, studies to date have been limited to AD/ MCI and HD/ premanifest HD; thirdly, none have taken a longitudinal approach; and finally, few of the studies related imaging findings to detailed neuropsychological/ cognitive testing. A great advantage of in vivo over post mortem studies is the ability to link imaging findings to the clinical syndromes experienced by patients. The relevance of studies which do not explore the relationship between imaging and clinical findings may be limited. It is likely that as 7T MRI becomes more widely available studies will include larger samples and produce longitudinal data,

allowing researchers to examine the changes seen as dementias develop and illuminating prognoses, e.g. by identifying which individuals with MCI will go on to develop AD.

In the small number of papers as yet published the predicted challenges of ultra-high resolution, such as increased artefact production, ghosting and image drop-out are not much commented upon in the papers. This implies that practical difficulties are less troublesome than the theory would suggest and that new technologies can overcome at least some of the issues. Total scan times were reported in 14 of the 19 papers reviewed and varied greatly according to the acquisition sequence used, FOV and voxel size. Increasing B_0 allows faster acquisition times or increased resolution; in these papers, authors have not consistently sought to draw on one or the other of these potential benefits. We may conclude that consensus on ideal imaging parameters at 7T in the dementia population has not yet been reached.

Of the papers reviewed only 3 reported on scan tolerability or adverse effects for subjects, despite the theoretical increased risks at 7T compared to lower field strengths. The low attrition rate in the studies and the lack of reported side effects may lead us to conclude that adverse effects were not often experienced by subjects in these studies. However, 7T MRI in vivo remains relatively new and the populations examined in the course of dementia research are likely to be among those who would be most at risk so ongoing vigilance is required.

The lack of in vivo 7T MRI studies investigating neurodegenerative dementias other than AD and HD is perhaps surprising, though a reminder that 7T is not widely available as yet. Results from AD studies suggest that 7T will be an important method for looking into LBD and FTD also. Like AD, LBD has much of its pathology in small, structurally complex and

often peripheral brain areas. Also somewhat surprising is the lack of papers taking a multi-modality approach, looking at correlations with PET, EEG or with systemic biological markers (other than APOE) such as immunological markers. Again, multi-modal studies are likely to be seen as 7T MRI becomes more widely available.

In summary, although 7T MRI is in its infancy it shows great promise for neurodegenerative dementia research. Looking to the future, the literature would benefit from larger cohorts, longitudinal data, greater correlation of imaging findings with the clinical picture and research into dementias other than AD and HD.

Acknowledgements:

The authors acknowledge the support of the Cambridge NIHR Biomedical Research Centre.

References:

1. Prince, M., Bryce, R., Albanese, E., Wimo, A., et al., 2013. The global prevalence of dementia: a systematic review and metaanalysis. *Alzheimers Dement.* 9(1):63-75
2. McKhann, G., Drachman, D., Folstein, M., et al., 1984. Clinical diagnosis of Alzheimer's disease: report of the NINCDS-ADRDA Work Group under the auspices of Department of Health and Human Services Task Force on Alzheimer's Disease. *Neurol.* 34(7):939-944
3. Braak, H., Braak, E., 1991. Neuropathological stageing of Alzheimer-related changes. *Acta Neuropathol.* 82(4):239-259
4. McKhann, G.M., Knopman, D.S., Chertkow, H., et al., 2011. The diagnosis of dementia due to Alzheimer’s disease: Recommendations from the National Institute on Aging- Alzheimer’s Association workgroups on diagnostic guidelines for Alzheimer’s disease. *Alzheimers Dement.* 7(3):263–269
5. Jack, C.R.Jr., Lowe, V.J., Senjem, M.L., et al., 2008. 11C PiB and structural MRI provide complementary information in imaging of Alzheimer’s disease and amnestic mild cognitive impairment. *Brain.* 131:665–680

6. Hampel, H., Bürger, K., Teipel, S.J., et al., 2008. Core candidate neurochemical and imaging biomarkers of Alzheimer's disease. *Alzheimers Dement.* 4(1):38-48
7. Zupancic, M., Mahajan, A., Handa, K., 2011. Dementia with lewy bodies: diagnosis and management for primary care providers. *Prim. Care Companion CNS Disord.* 13(5)
8. McKeith, I.G., Dickson, D.W., Lowe, J,. et al., 2005. Diagnosis and management of dementia with Lewy bodies: third report of the DLB Consortium. Neurol. 65(12):1863-1872
9. Papathanasiou, N.D., Boutsiadis, A., Dickson, J., Bomanji, J.B., 2012. Diagnostic accuracy of ^{123}I-FP-CIT (DaTSCAN) in dementia with Lewy bodies: a meta-analysis of published studies. *Parkinsonism Relat. Disord.* 18(3):225-229
10. Mak, E., Su, L., Williams, G.B et al., 2014. Neuroimaging characteristic of dementia with Lewy bodies. *Alzheimer's Res. Therapy.* 6:18
11. Rohrer, J.D., 2012. Structural brain imaging in frontotemporal dementia. *Biochim. Biophys. Acta.* 1822:325–332
12. Pringsheim, T., Wiltshire, K., Day, L., et al., 2012. The Incidence and Prevalence of Huntington's Disease: A Systematic Review and Meta-analysis. *Movement Disord.* 27(9):1083-1091
13. Vonsattel, JP.G., DiFiglia, M., 1998. Huntington Disease. *J. Neuropathol. Exp. Neurol.* 57(5)369-384
14. Niccolini, F., Politis, M., 2014. Neuroimaging in Huntington's disease. *World J. Radiol.* 6(6):301-312
15. Tabrizi, S.J., Reilmann, R., Roos, R.A.C., et al., 2012. Potential endpoints for clinical trials in premanifest and early Huntington's disease in the TRACK-HD study: analysis of 24 month observational data. *Lancet Neurol.* 11:42–53
16. NICE-SCIE Dementia., 2007 (updated 2011). The NICE-SCIE Guideline on Supporting People with Dementia and their Carers in Health and Social Care. http://www.scie.org.uk/publications/misc/dementia/dementia-fullguideline.pdf?res=true (accessed 03.06.16)
17. Chow, N., Hwang, K.S., Hurtz, S., et al., 2015. Comparing 3T and 1.5T MRI for Mapping Hippocampal Atrophy in the Alzheimer's Disease Neuroimaging Initiative. *Am. J. Neuroradiol.* 36(4):653-660
18. Balchandani, P., Naidich, T.P., 2015. Ultra-High-Field MR Neuroimaging. *Am. J. Neuroradiol.* 36(7):1204-1215

19. Moseley, M.E., Liu, C., Rodriguez, S., et al., 2009. Advances in Magnetic Resonance Neuroimaging. *Neurol. Clin.* 27(1):1–xiii
20. Perl, D.P., 2010. Neuropathology of Alzheimer's disease. *Mt. Sinai J. Med.* 77(1):32-42
21. Medicines and Healthcare Products Regulatory Agency., 2015. Safety Guidelines for Magnetic Resonance Imaging Equipment in Clinical Use. https://www.gov.uk/government/uploads/system/uploads/attachment_data/file/476931/MRI_guidance_2015_-_4-02d1.pdf (assessed 02.06.16)
22. Health Protection Agency., 2008. Protection of Patients and Volunteers Undergoing RI Procedures. Documents of the Health Protection Agency Radiation, Chemical and Environmental Hazards. https://www.gov.uk/government/uploads/system/uploads/attachment_data/file/329364/Protection_of_patients_and_volunteers_undergoing_MRI_procedures.pdf (accessed 02.06.16)
23. Albert, M.S., DeKosky, S.T., Dickson, D., et al., 2011. The diagnosis of mild cognitive impairment due to Alzheimer's disease: recommendations from the National Institute on Aging-Alzheimer's Association workgroups on diagnostic guidelines for Alzheimer's disease. *Alzheimers Dement.* 7(3):270-279
24. Petersen, R.C., Smith, G.E., Waring, S.C., et al., 1999. Mild cognitive impairment: clinical characterization and outcome. *Arch. Neurol.* 56(3):303-308
25. Boutet, C., Chupin, M., Lehéricy, S., et al., 2014. Detection of volume loss in hippocampal layers in Alzheimer's disease using 7 T MRI: a feasibility study. *Neuroimage Clin.* 5:341-348
26. Kerchner, G.A., Hess, C.P., Hammond-Rosenbluth, K.E., et al., 2010. Hippocampal CA1 apical neuropil atrophy in mild Alzheimer disease visualized with 7-T MRI. *Neurol.* 75:1381–1387
27. Kerchner, G.A., Deutsch, G.K., Zeineh, M., et al., 2012. Hippocampal CA1 apical neuropil atrophy and memory performance in Alzheimer's disease. *NeuroImage.* 63(1):194-202
28. Kerchner, G.A., Bernstein, J.D., Fenesy, M.C., et al., 2013. Shared vulnerability of two synaptically-connected medial temporal lobe areas to age and cognitive decline: a seven tesla magnetic resonance imaging study. *J. Neurosci.* 33(42):16666-16672
29. Kerchner, G.A., Berdnik, D., Shen, J.C., et al., 2014. APOE ε4 worsens hippocampal CA1 apical neuropil atrophy and episodic memory. *Neurol.* 82(8):691-697

30. Wisse, L.E., Biessels, G.J., Heringa, S.M., et al., 2014. Hippocampal subfield volumes at 7T in early Alzheimer's disease and normal aging. *Neurobiol. Aging.* 35(9):2039-2045
31. Wisse, L.E., Reijmer, Y.D., ter Telgte, A., et al., 2015. Hippocampal disconnection in early Alzheimer's disease: a 7 tesla MRI study. *J. Alzheimers Dis.* 45(4):1247-1256
32. Brundel, M., Heringa, S.M., de Bresser, J., et al., 2012b. High prevalence of cerebral microbleeds at 7Tesla MRI in patients with early Alzheimer's disease. *J. Alzheimers Dis.* 31(2):259-263
33. Gregoire, S.M., Chaudhary, U.J., Brown, M.M., et al., 2009. The Microbleed Anatomical Rating Scale (MARS): Reliability of a tool to map brain microbleeds. *Neurol.* 73:1759-1766
34. van Veluw, S.J., Heringa, S.M., Kuijf, H.J., et al., 2014. Cerebral Cortical Microinfarcts at 7Tesla MRI in Patients with Early Alzheimer's Disease. *J. Alzheimer's Dis.* 39:163–167
35. Van Veluw SJ, Zwanenburg JJ, Engelen-Lee J, et al. In vivo detection of cerebral cortical microinfarcts with high-resolution 7T MRI. J Cereb Blood Flow Metab 2013;33:322-329.
36. Nakada, T., Matsuzawa, H., Igarashi, H., et al., 2008. In vivo visualization of senile-plaque-like pathology in Alzheimer's disease patients by MR microscopy on a 7T system. *J. Neuroimaging.* 18(2):125-9
37. Nakada, T., 2007. Clinical application of high and ultra high-field MRI. *Brain Dev.* 29:325-335
38. van Bergen, J.M.G., Li, X., Hua, J., et al., 2016a. Colocalization of cerebral iron with Amyloid beta in Mild Cognitive Impairment. *Nature Scientific Reports* 6:35514
39. Li, W., Wu, B., Liu, C., 2011. Quantitative susceptibility mapping of human brain reflects spatial variation in tissue composition. *NeuroImage.* 55:1645–1656
40. van Rooden, S., Versluis, M.J., Liem, M.K., et al., 2014. Cortical phase changes in Alzheimer's disease at 7T MRI: a novel imaging marker. *Alzheimers Dement.* 10(1):e19-26
41. van Rooden, S., Doan, N.T., Versluis, M.J., et al., 2015. 7T T_2*-weighted magnetic resonance imaging reveals cortical phase differences between early- and late-onset Alzheimer's disease. *Neurobiol. Aging.* 36(1):20-26
42. Cai, K., Tain, R., Das, S., et al., 2015. The feasibility of quantitative MRI of perivascular spaces at 7T. *J. Neurosci. Methods.* 256:151-156

43. Versluis, M.J., Peeters, J.M., van Rooden, S., et al., 2010. Origin and reduction of motion and f0 artifacts in high resolution T2*-weighted magnetic resonance imaging: Application in Alzheimer's disease patients. *NeuroImage.* 51:1082–1088
44. Serrano-Pozo, A., Mielke, M.L., Muzitansky, A., et al., 2012. Stable Size Distribution of Amyloid Plaques Over the Course of Alzheimer Disease. *J. Neuropathol. Exp. Neurol.* 71(8):694-701
45. Apple, A.C., Possin, K.L., Satris, G., et al., 2014. Quantitative 7T phase imaging in premotor Huntington disease. *Am. J. Neuroradiol.* 35(9):1707-1713
46. Hammond, K.E., Lupo, J.M., Xu, D., et al., 2008. Development of a robust method for generating 7.0 T multichannel phase images of the brain with application to normal volunteers and patients with neurological diseases. *Neuroimage.* 39:1682–1692
47. van Bergen, J.M.G., Hua, J., Unschuld, P.J., et al., 2016b. Quantitative susceptibility mapping suggests altered brain iron in premanifest Huntington's disease. *Am. J. Neuroradiol.* 37(5):789-796
48. Deistung, A., Schafer, A., Schweser, F., et al., 2013. Toward in vivo histology: a comparison of quantitative susceptibility mapping (QSM) with magnitude-, phase-, and R2*-imaging at ultra-high magnetic field strength. *NeuroImage.* 65:299–314
49. Doan, N.T., van den Bogaard, S.J.A., Dumas, E.M., et al., 2014. Texture Analysis of Ultrahigh Field T2*-Weighted MR Images of the Brain: Application to Huntington's Disease. *J. Mag. Reson. Image.* 39:633–640
50. Chen, W., Giger, M.L., Li, H., et al., 2007. Volumetric texture analysis of breast lesions on contrast-enhanced magnetic resonance images. *Magn. Reson. Med.* 58:562–571
51. Drouin-Ouellet, J., Sawiak, S.J., Cisbani, G., et al., 2015. Cerebrovascular and Blood–Brain Barrier Impairments in Huntington's Disease: Potential Implications for Its Pathophysiology. *Ann. Neurol.* 78:160–177
52. Francis, S.T., Bowtell, R., Gowland, P.A., 2008. Modeling and optimization of Look-Locker spin labeling for measuring perfusion and transit time changes in activation studies taking into account arterial blood volume. *Magn. Reson. Med.* 59:316–325
53. Huntington Study Group, 1996. Unified Huntington's Diesease Rating Scale: reliability and consistency. *Movement Disord. Soc.* 11(2):136-142

54. Zhang, Y., Long, J.D., Mills, J.A., et al., 2011. Indexing disease progression at study entry with individuals at-risk for Huntington disease. *Am. J. Med. Genet. B. Neuropsychiatr. Genet.* 156B(7):751-63
55. Duvernoy, H.M., Cattin, E., Naidich, T., et al., 2005. The Human Hippocampus, third ed. Springer, Berlin, pp. 1e232
56. Price, J.L., Ko, A.I., Wade, M.J., et al., 2001. Neuron number in the entorhinal cortex and CA1 in preclinical Alzheimer disease. *Arch. Neurol.* 58:1395-1402
57. Frisoni, G.B., Fox, N.C., Jack, C.R., et al., 2010. The clinical use of structural MRI in Alzheimer disease. *Nat. Rev. Neurol.* 6(2): 67–77
58. Stucht, D., Danishad, K.A., Schulze, P., et al., 2015. Highest Resolution In Vivo Human Brain MRI Using Prospective Motion Correction. *PLoS ONE* 10(7):e0133921
59. Fox, N.C., Cousens, S., Scahill, R.A., et al., 2000. Using Serial Registered Brain Magnetic Resonance Imaging to Measure Disease Progression in Alzheimer Disease: Power Calculations and Estimates of Sample Size to Detect Treatment Effects. *Arch. Neurol.* 57(3):339-344
60. Bertrand, E., Lechowicz, W., Lewandowska, E., et al., 2003. Degenerative axonal changes in the hippocampus and amygdala in Parkinson's disease. *Folia Neuropathol.* 41(4):197-207
61. Chow, N., Aarsland, D., Honarpisheh, H., et al., 2012. Comparing hippocampal atrophy in Alzheimer's dementia and Dementia with Lewy Bodies. *Dement. Geriatr. Cogn. Disord.* 34(1): 44–50
62. Mak, E., Su, L., Williams, G.B., et al., 2016. Differential Atrophy of Hippocampal Subfields: A Comparative Study of Dementia with Lewy Bodies and Alzheimer Disease. *Am. J. Geriatr. Psychiatry.* 24(2):136-143
63. Deuker, L., Doeller, C.F., Fell, J., et al., 2014. Human neuroimaging studies on the hippocampal CA3 region – integrating evidence for pattern separation and completion. *Front. Cell. Neurosci.* 8:64
64. Rabinovici, G.D., Jagust, W.J., 2009. Amyloid imaging in aging and dementia: testing the amyloid hypothesis in vivo. *Behav. Neurol.* 21:117–128
65. Meadowcroft, M.D., Connor, J.R., Smith, M.B., et al., 2009. MRI and Histological Analysis of Beta-Amyloid Plaques in Both Human Alzheimer’s Disease and APP/PS1 Transgenic Mice. *J. Mag. Reson. Image.* 29:997–1007

66. Zeineh, M.M., Chen, Y., Kitzler, H.H., et al., 2015. Activated iron-containing microglia in the human hippocampus identified by magnetic resonance imaging in Alzheimer disease. *Neurobiol. Aging* 36:2483-2500
67. Connor, J.R., Menzies, S.L., St. Martin, S.M., et al., 1992. Histochemical study of iron, transferrin, and ferritin in Alzheimer's diseased brains. *J. Neurosci. Res.* 31:75-83
68. Sian-Hülsmann, J., Mandel, S., Youdim, M.B., et al., 2011. The relevance of iron in the pathogenesis of Parkinson's disease. *J. Neurochem.* 118(6):939-57
69. Gazzina, S., Premi, E., Zanella, I., et al., 2016. Iron in Frontotemporal Lobar Degeneration: A New Subcortical Pathological Pathway. *Neurodegener. Dis.* 16(3-4):172-8
70. Conijn, M.M.A., Geerlings, M.I., Biessels, G.J., et al., 2011. Cerebral Microbleeds on MR Imaging: Comparison between 1.5 and 7T. *Am. J. Neuroradiol.* 32:1043–1049
71. Cordonnier, C., van der Flier, W.M., 2011. Brain microbleeds and Alzheimer's disease: Innocent observation or key player? *Brain.* 134:335-344
72. Brundel, M., de Bresser, J., van Dillen, J.J., et al., 2012a. Cerebral microinfarcts: a systematic review of neuropathological studies. *J. Cereb. Blood Flow Metab.* 32(3):425-436
73. Muller, M., Leavitt, B.R., 2014. Iron dysregulation in Huntington's disease. *J. neurochem.* 130:328-350
74. Langkammer, C., Ropele, S., Pirpamer, L., et al., 2014. MRI for iron mapping in Alzheimer's disease. *Neurodegener. Dis.* 13(2-3):189-91
75. Nelson, P.T., Jicha, G.A., Kryscio, R.J., et al., 2010. Low sensitivity in clinical diagnoses of dementia with Lewy bodies. *J. Neurol.* 257(3):359–366
76. Calamante, F., Oh, S.H., Tournier, J.D., et al., 2013. Super-resolution track-density imaging of thalamic substructures: comparison with high-resolution anatomical magnetic resonance imaging at 7.0T. *Hum. Brain Mapp.* 34(10):2538-2548
77. Warren, J.D., 2013. Frontotemporal dementia. *BMJ* 347:f4827
78. Whitwell, J.L., Josephs, K.A., 2012. Recent Advances in the Imaging of Frontotemporal Dementia. *Curr. Neurol. Neurosci. Rep.* 12(6):715–723